Genomics Characterization of an Engineered *Corynebacterium glutamicum* in Bioreactor Cultivation Under Ionic Liquid Stress

Deepanwita Banerjee[1,2†], Thomas Eng[1,2†], Yusuke Sasaki[1,2], Aparajitha Srinivasan[1,2], Asun Oka[2,3], Robin A. Herbert[1,2], Jessica Trinh[1,2], Vasanth R. Singan[2,4], Ning Sun[2,3], Dan Putnam[5], Corinne D. Scown[1,6], Blake Simmons[1,2] and Aindrila Mukhopadhyay[1,2]*

[1]Joint BioEnergy Institute, Lawrence Berkeley National Laboratory, Emeryville, CA, United States, [2]Biological Systems and Engineering Division, Lawrence Berkeley National Laboratory, Berkeley, CA, United States, [3]Advanced Biofuels and Bioproducts Process Development Unit, Lawrence Berkeley National Laboratory, Emeryville, CA, United States, [4]Joint Genome Institute, Lawrence Berkeley National Laboratory, Berkeley, CA, United States, [5]Department of Plant Sciences, University of California, Davis, Davis, CA, United States, [6]Energy Analysis and Environmental Impacts Division, Lawrence Berkeley National Laboratory, Berkeley, CA, United States

Corynebacterium glutamicum is an ideal microbial chassis for production of valuable bioproducts including amino acids and next generation biofuels. Here we resequence engineered isopentenol (IP) producing *C. glutamicum* BRC-JBEI 1.1.2 strain and assess differential transcriptional profiles using RNA sequencing under industrially relevant conditions including scale transition and compare the presence *vs* absence of an ionic liquid, cholinium lysinate ([Ch][Lys]). Analysis of the scale transition from shake flask to bioreactor with transcriptomics identified a distinct pattern of metabolic and regulatory responses needed for growth in this industrial format. These differential changes in gene expression corroborate altered accumulation of organic acids and bioproducts, including succinate, acetate, and acetoin that occur when cells are grown in the presence of 50 mM [Ch][Lys] in the stirred-tank reactor. This new genome assembly and differential expression analysis of cells grown in a stirred tank bioreactor clarify the cell response of an *C. glutamicum* strain engineered to produce IP.

Keywords: *Corynebacterium glutamicum*, RNAseq, fed-batch, bioreactor, ionic Liquid, isopentenol, acetoin, lignin hydrolysate

INTRODUCTION

Due to process advantages, biological methods for the production of amino acids over chemical synthesis methods fostered the identification of natural glutamine overproducing microbes (Kinoshita et al., 1958). Since then, *Corynebacterium glutamicum* has been used successfully to produce specialty glutamine and specialty amino acids to meet global demand. The advent of accessible whole-genome sequencing and mutagenesis methods have enabled a clearer understanding of how specific isolates can overproduce these desired molecules, as well as how they maintain productivity across volumetrically-larger scales (Becker et al., 2018; Pérez-García and Wendisch, 2018; Wolf et al., 2021). Using *C. glutamicum* to produce non-native metabolites as next-generation biofuels is an attractive large-volume market with the potential to reduce global carbon emissions. Potential biofuels can be produced from terpenes, which use different metabolic

FIGURE 1 | Growth and isopentenol production characterization of two genetically distinct engineered *C. glutamicum* strains, **(A)** Isopentenol (IP) production in *C. glutamicum* strains of the genotypes indicated harboring an IP production plasmid. Cells were cultivated in 24-well deep well plates. IP titers reported at 48-h time points are corrected for evaporation in this plate format (Materials and Methods), **(B)** Growth curves for *C. glutamicum* strains of the indicated strain backgrounds cultivated in CGXII media in the presence or absence of the IL, cholinium lysinate ([Ch][Lys]), [Ch][Lys] was exogenously added to the culture media at the start of the time course, **(C)** Production of IP from *C. glutamium* grown in CGXII minimal media with pure glucose (4% w/v) or ensiled [Ch][Lys] pretreated sorghum hydrolysate. An optimized IP production plasmid carrying a *hmgR* variant from *Silicibacter pomeroyi* was used. The optical density of cultures as a proxy for cell density is noted on the right-hand panel.

precursors (reviewed in (Pérez-García and Wendisch, 2018)). We have previously described the heterologous expression of the terpenoid isopentenol (IP; also known as 3-methyl-3-buten-1-ol or isoprenol) pathway in *C. glutamicum* (Sasaki et al., 2019). IP can be used directly as a drop-in biogasoline (Reninger and McPhee, 2008; Chou and Keasling, 2012) or as a precursor to a jet fuel, DMCO (Baral et al., 2021). Producing IP was improved using optimal pathway homologs, specific media formulation and aeration conditions and an empirically determined carbon/nitrogen ratio (Sasaki et al., 2019).

In this study we build upon this established system to analyze the behavior of *C. glutamicum* strains engineered to produce IP in a bioreactor. The bioreactor cultivation and process conditions can provide key diagnostic information essential to build robust production platform strains (Wehrs et al., 2019). In addition, it is also valuable to understand microbial response to the carbon

feedstock that is anticipated for actual production. Here, we explore the use of plant-based lignocellulosic hydrolysate generated using ionic liquid (IL) as a pretreatment reagent. Toxicity from residual pretreatment reagents such as ILs is a known source of growth impediment (Hou et al., 2013; Santos et al., 2014). *C. glutamicum* is tolerant to many ILs, another attribute that makes it an ideal host for biomass conversion (Sasaki et al., 2019). In this study, we characterize an IP-producing engineered *C. glutamicum* strain with long-read Pacific Biosciences (PacBio) whole-genome sequencing. This high-quality assembly allowed accurate mapping for differential RNA expression analysis from a diagnostic fed-batch *C. glutamicum* IP production run. These side-by-side experiments characterize the cellular response to the IL, cholinium lysinate ([Ch][Lys]), when grown in a fed-batch stirred tank bioreactor.

RESULTS

Characterization of Isopentenol Production and Ionic Liquid Tolerance in *C. glutamicum* Strains

We established that the strain reported in Sasaki et al., 2019, *C. glutamicum* (previously referred to as ATCC 13032 NHRI 1.1.2) outperformed another isolate, ATCC 13032 Δ*cglIM* Δ*cgLIR* Δ*cgLIIR* (referred to as "Δ*mrr*") (**Figure 1A**). *C. glutamicum* Δ*mrr* was first described in Baumgart et al., 2013 and is a methylation-deficient strain widely used due to its improved plasmid transformation and genomic integration rate (Schäfer et al., 1997; Baumgart et al., 2013). When *C. glutamicum* BRC-JBEI 1.1.2 is used in conjunction with an IP production pathway, it can produce 300 mg/L IP from pure glucose, but the product titers are near the lower detection limit by GC-FID in the *C. glutamicum* ATCC 13032 Δ*mrr* strain. While only *C. glutamicum* BRC-JBEI 1.1.2 produced IP, both the type strain and this specific isolate tolerate high concentrations of exogenous ILs (**Figure 1B**), suggesting that IL tolerance was a shared feature between these two isolates despite differences in IP production.

We also confirmed the ability of *C. glutamicum* BRC-JBEI 1.1.2 to handle renewable carbon streams from sorghum biomass using an improved carbon extraction protocol enhanced by the use of ensiled biomass (Magurudeniya et al., 2021). The ensiling process enables naturally occurring lactic-acid secreting bacteria to partially decompose the hemicellulose in sorghum while stored in a silo before downstream processing. After ensiling, the biomass was pretreated with [Ch][Lys] followed by enzymatic saccharification (Materials and Methods). This hydrolysate contained 48.7 g/L glucose, 17.9 g/L xylose, and trace concentrations of aromatic compounds. Our optimized *C. glutamicum* BRC-JBEI 1.1.2 with an optimized IP production system had no detected growth defects when grown with 58% (v/v) hydrolysate supplemented media and produced 1 g/L IP from pure glucose or ~600 mg/L IP from sorghum hydrolysate (**Figure 1C**). These results showcase its versatility with handling actual plant biomass derived carbon streams. For the remainder of this study, we focus on characterizing the genetic differences present in *C. glutamicum* BRC-JBEI 1.1.2 relative to other closely related *C. glutamicum* strains that might explain the IP production values between these two strains.

Genomic Characterization of *C. glutamicum* BRC-JBEI 1.1.2

While 16S rRNA sequencing suggested that *C. glutamicum* Δ*mrr* strain as in the *C. glutamicum* ATCC 13032 strain background, this same method indicated that *C. glutamicum* BRC-JBEI 1.1.2 is related to *C. glutamicum* CICC10112 or SCgG1/SCgG2. To overcome the limitation inherent to 16S rRNA-based identification, we turned to using whole genome sequencing. Only SCgG1 and SCgG2 have been characterized with whole-genome sequencing, and to our knowledge there was no additional information about *C. glutamicum* CICC10112 beyond the partial 16S ribosomal sequence. As 16S rRNA is

inconclusive for isolate-level identification (Sabat et al., 2017; Hahne et al., 2018; Johnson et al., 2019), we reasoned that the whole-genome sequencing in this IP producing strain would ensure an accurate reference genome in downstream RNAseq analysis if the improved performance observed in this strain was due to variations in the strain background. One of the major limitations in short-read sequencing is the difficulty in assembling overlapping contigs to generate a high-quality *de novo* assembly of a single contiguous read. Therefore, we chose PacBio long-read sequencing (Koren and Phillippy, 2015) for optimal coverage over short read sequencing as a potential solution. However, routine methods for lysing and isolating *C. glutamicum* genomic DNA were insufficient for building high-quality genome assemblies since the physical lysis method we employed (Eng et al., 2018) shears DNA to fragments ranging from 2 to 8 kb in size. Detergent-based lysis methods failed to extract genomic DNA, even with prolonged incubation times. We developed a method to isolate larger DNA fragments approximately 20 kb in size for the PacBio Sequel (Pacific Biosciences) assembly pipeline using a zymolyase protease treatment for cell lysis (see Materials and Methods). This modified DNA extraction protocol enabled us to use PacBio long read sequencing to generate a high-quality *de novo* genome assembly.

We now report a new genome assembly of a single contiguous scaffold of 3,352,276 bases with 53.83% GC content (**Figure 2**). Genome-wide average nucleotide identity (ANI) confirmed this isolate was 99.9987% identical to *C. glutamicum* SCgG1 and SCgG2 as well as another sequenced *C. glutamicum* isolate, Z188. The average nucleotide identity alignment for the 28 sequenced *C. glutamicum* isolates has been deposited at the database of the Joint Genome Institute (https://genome.jgi.doe.gov/portal/), Project ID 1203597 and is also included in **Supplementary Table S1**. *C. glutamicum* BRC-JBEI 1.1.2 differs from SCgG1 only by a few single nucleotide polymorphisms (~10) and two additional genes that are absent from SCgG1, a putative transposase and a hypothetical protein coding sequence that is 414 bp in length. When *C. glutamicum* BRC-JBEI 1.1.2 was compared with more commonly used reference strains, *C. glutamicum* R and 13032 (Bielefeld), we identified genomic islands encoding genes unique to BRC-JBEI 1.1.2. Genome topology analysis also identified a 140 kb inversion in the genome of BRC-JBEI 1.1.2 isolate (**Figure 2A**). Out of 3,097 genes, homology mapping indicated that 85% (2,641 genes) were at least 80% identical to known genes in *C. glutamicum* ATCC 13032. With a less restrictive % identity threshold of 50%, the identical ratio could account for 89% (2,777 genes). Nonetheless, 320 genes did not meet the minimum % identity threshold and could not be annotated with this reference genome (**Supplementary Figure S1**).

Some of these unknown genes that were unique to BRC-JBEI 1.1.2 might be related to the catabolism of IL. Intriguingly, a putative choline dehydrogenase, *Ga0373873_2846*, showed only 40% identity to other known choline dehydrogenases primarily found in Gram-negative microbes such as *Burkholderia phytofirmans* PsJN and *Cupriavidus basilensis* FW507-4G11. Meta-COG analysis of these four *C. glutamicum* genomes
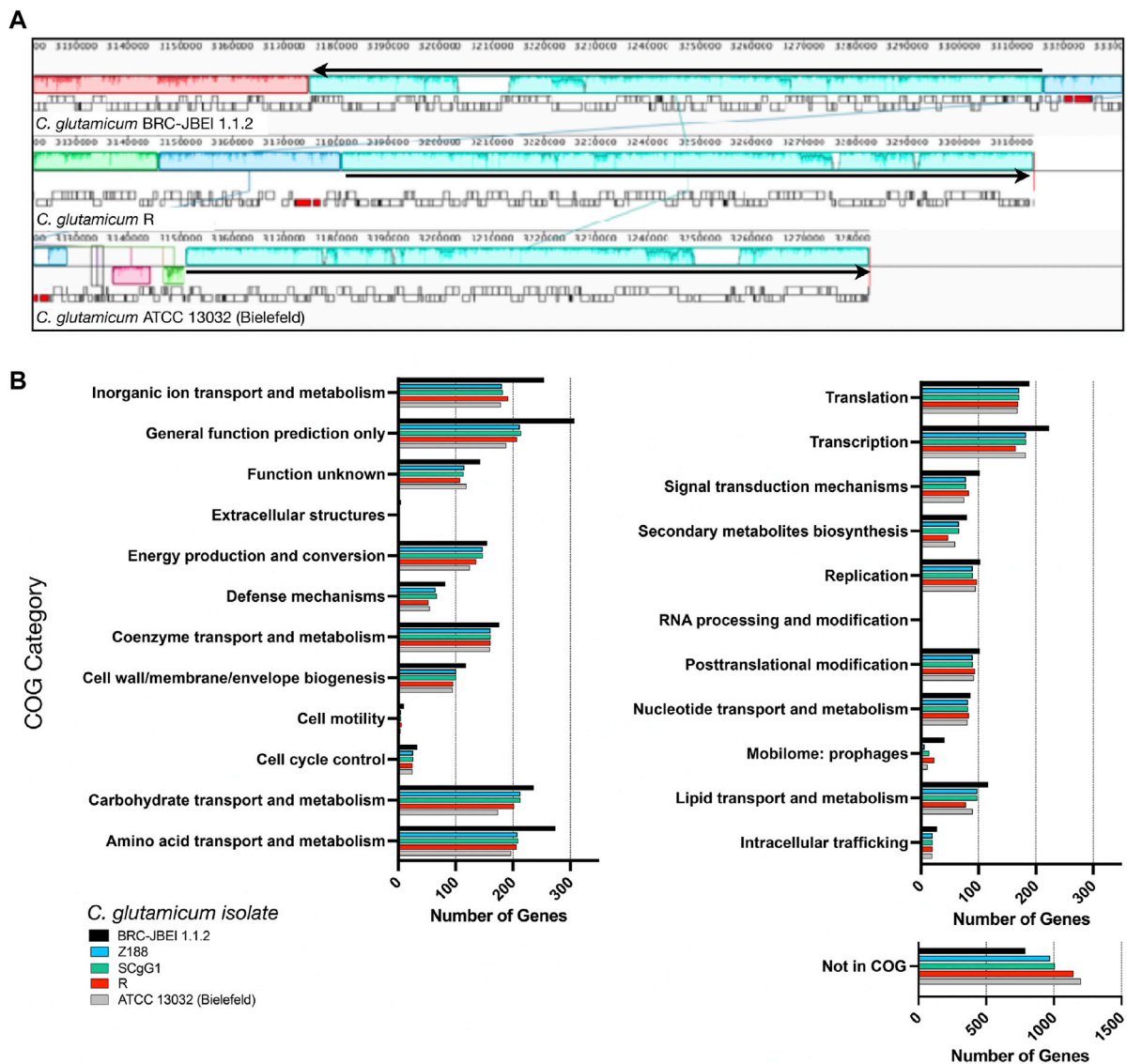
FIGURE 2 | Comparison of the *C. glutamicum* BRC-JBEI 1.1.2 strain with closely related *C. glutamicum* strains, **(A)** A meta-analysis of gene function using clusters of orthologous genes (COGs) analysis. The total number of genes in each category for each strain is represented with colored bars as indicated, **(B)** Mauve genome alignment of *C. glutamicum* BRC-JBEI 1.1.2 with *C. glutamicum* R and 13032 (Bielefeld). Similar genomic regions share the same color across the three different genomes compared. A 140 kb chromosomal inversion is highlighted in light blue, and the relative direction of the inversion in each strain is indicated with a black arrow. Individual genes are indicated with open rectangles underneath the colored area.

revealed that *C. glutamicum* BRC-JBEI 1.1.2 contains over 100 additional genes related to the transport or metabolism of inorganic ions, carbohydrates, and amino acids, suggesting a broader metabolic capacity to utilize a more significant number of substrates than the type strain (**Figure 2**). In summary, this genome sequencing analysis was valuable for characterizing differences between *C. glutamicum* BRC-JBEI 1. 1.2 and the more routinely studied type strain ATCC 13032. Due to its similarity with SCgG1 and SCgG2, *C. glutamicum* BRC-JBEI 1.1.2 is likely an industrial glutamate overproducing isolate but has more annotations in the inorganic ion and amino acid transport and metabolism COG categories than its nearest

neighbors, SCgG1, SCgG2, and Z188 that need further characterization.

Transcriptome Analysis Identifies Changes in *C. glutamicum* Beyond Metabolism During Scale-Up

Next, we sought to build a systems-level understanding of *C. glutamicum* gene expression changes in bioreactors upon exogenous IL treatment. This data could be useful for subsequent Design-Build-Test-Learn (DBTL) cycles in providing the diagnostic information for future strain optimization strategies
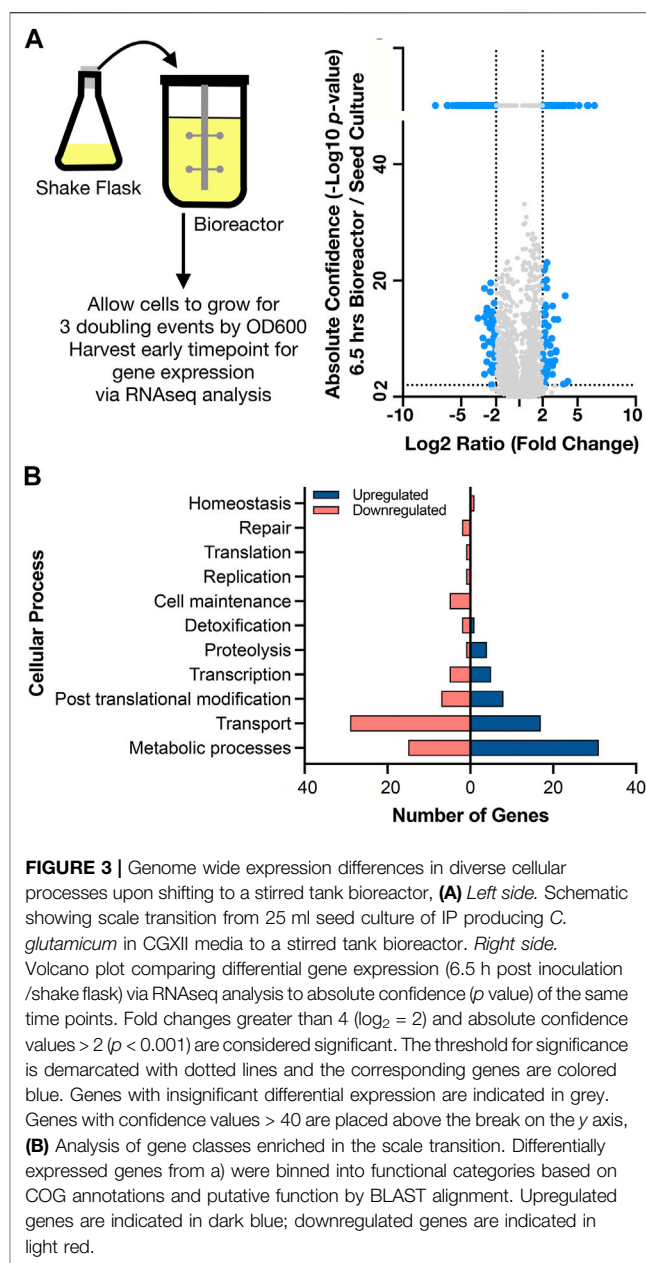
(Opgenorth et al., 2019). We prepared samples from sequential time points during a scaleup campaign to analyze shifts in gene expression as a proxy for changes in metabolic and regulatory behavior in both [Ch][Lys] treated and untreated runs. First, we determined if the failure to produce IP was due to loss of the production pathway, possibly due to loss of the plasmid-borne IP pathway genes. The IP production pathway is composed of 5 genes in 2 adjacent operons under the *trc* and *lacUV5* promoters, namely *mk, pmd* and *atoB, hmgS, hmgR* respectively. Using the transcripts per million (TPM) metrics, we examined absolute gene expression levels as well as changes over the course of the production campaign. The IP pathway started off high for both *hmgR* and *hmgS* in the shake flask (200,000 TPM), but expression of these two genes decreased between 10-16x over the duration of the 65-h fed batch. Expression amounts of *atoB* in the shake flask were comparatively lower (1,500 TPM) but decreased 4x at the shake flask to bioreactor transition. *atoB* TPM counts remained low for the duration of the subsequent time points. Since the pathway genes were still expressed during this run, we then focused on analyzing gene expression changes in the native *C. glutamicum* genome.

To interpret the differential gene expression results with genes identified in the new assembly for *C. glutamicum* BRC-JBEI 1.1.2, we mapped gene names and identifiers from *C. glutamicum* ATCC 13032 back onto the open reading frames (ORFs) in *C. glutamicum* BRC-JBEI 1.1.2 as genes in the type strain genome have been broadly characterized. We used a medium confidence cutoff of 70% identity to capture most homologs when analyzing this dataset. First, we characterised gene expression upon inoculating cells from the seed culture in a shake flask to the bioreactor. This differential gene expression (DEG) was calculated as the ratio of an early time point in the bioreactor (6.5 h post inoculation in the stirred tank) divided by values from the seed culture immediately before transfer. This time point was chosen to give cells approximately three doublings to ensure the cells were rapidly growing under these new conditions. The result showed differential expression of 258 genes after 6.5 h (**Figure 3**, and **Supplementary Dataset S1**).

Overexpressed Metabolic Genes

Many genes encoding metabolic functions were differentially expressed in the transition from shake flask to stirred tank format. We used a fold change cutoff of 4 ($\log_2 > 2$) and a *p* value < 0.001 to identify both large and statistically significant changes (**Figure 3A**). Gene ontology (GO) (Ashburner et al., 2000) enrichment annotations identified the highest number of DEGs belonging to metabolism and transport processes (**Figure 3B**). The strongest fold changes (16-fold increase or higher) were in metabolism; Cgl2807 (*adhA*, zinc dependent alcohol dehydrogenase), Cgl1396 (acetylglutamate kinase), Cgl2886 and Cgl2887 (two FAD-dependent oxidoreductases) and Cgl3007 (*mez*, malic enzyme). Of these genes, Cgl2807/ *adhA* encodes for a Zn-dependent alcohol dehydrogenase that together with Cgl2796 has been reported to maintain redox balance (Zhang et al., 2018). While the cells had been previously adapted in CGXII medium for the seed culture, we observed differentially increased gene expression of several amino acid biosynthesis pathways. Increased gene expression for nearly complete pathways needed for methionine, leucine, and arginine

FIGURE 3 | Genome wide expression differences in diverse cellular processes upon shifting to a stirred tank bioreactor, **(A)** *Left side.* Schematic showing scale transition from 25 ml seed culture of IP producing *C. glutamicum* in CGXII media to a stirred tank bioreactor. *Right side.* Volcano plot comparing differential gene expression (6.5 h post inoculation /shake flask) via RNAseq analysis to absolute confidence (*p* value) of the same time points. Fold changes greater than 4 ($\log_2 = 2$) and absolute confidence values > 2 (*p* < 0.001) are considered significant. The threshold for significance is demarcated with dotted lines and the corresponding genes are colored blue. Genes with insignificant differential expression are indicated in grey. Genes with confidence values > 40 are placed above the break on the *y* axis, **(B)** Analysis of gene classes enriched in the scale transition. Differentially expressed genes from a) were binned into functional categories based on COG annotations and putative function by BLAST alignment. Upregulated genes are indicated in dark blue; downregulated genes are indicated in light red.

biosynthesis were detected, as well as the gene responsible for glutamate synthesis, *gdh*. Three genes responsible for the conversion of propionate to succinate and pyruvate through the methylcitrate cycle were also upregulated. Upregulated DEGs encoding for myo-inositol metabolism directing flux towards acetyl-CoA and DHAP included Cgl0163/*iolE*, Cgl0161/*iolB*, Cgl0158/*iolC*, Cgl0160/*iolA/msmA*, and Cgl0157/ *iolR*. Of the myo-inositol pathway genes, *iolR* was reported to regulate PTS-independent glucose uptake by repressing the expression of glucokinases in *C. glutamicum* (Zhou et al., 2015). The upregulation of myo-inositol catabolic pathways could be attributed to supplemental yeast extract amended to the CGXII medium in the bioreactor. Yeast extract was added to the bioreactors as it was found to improve IP production in
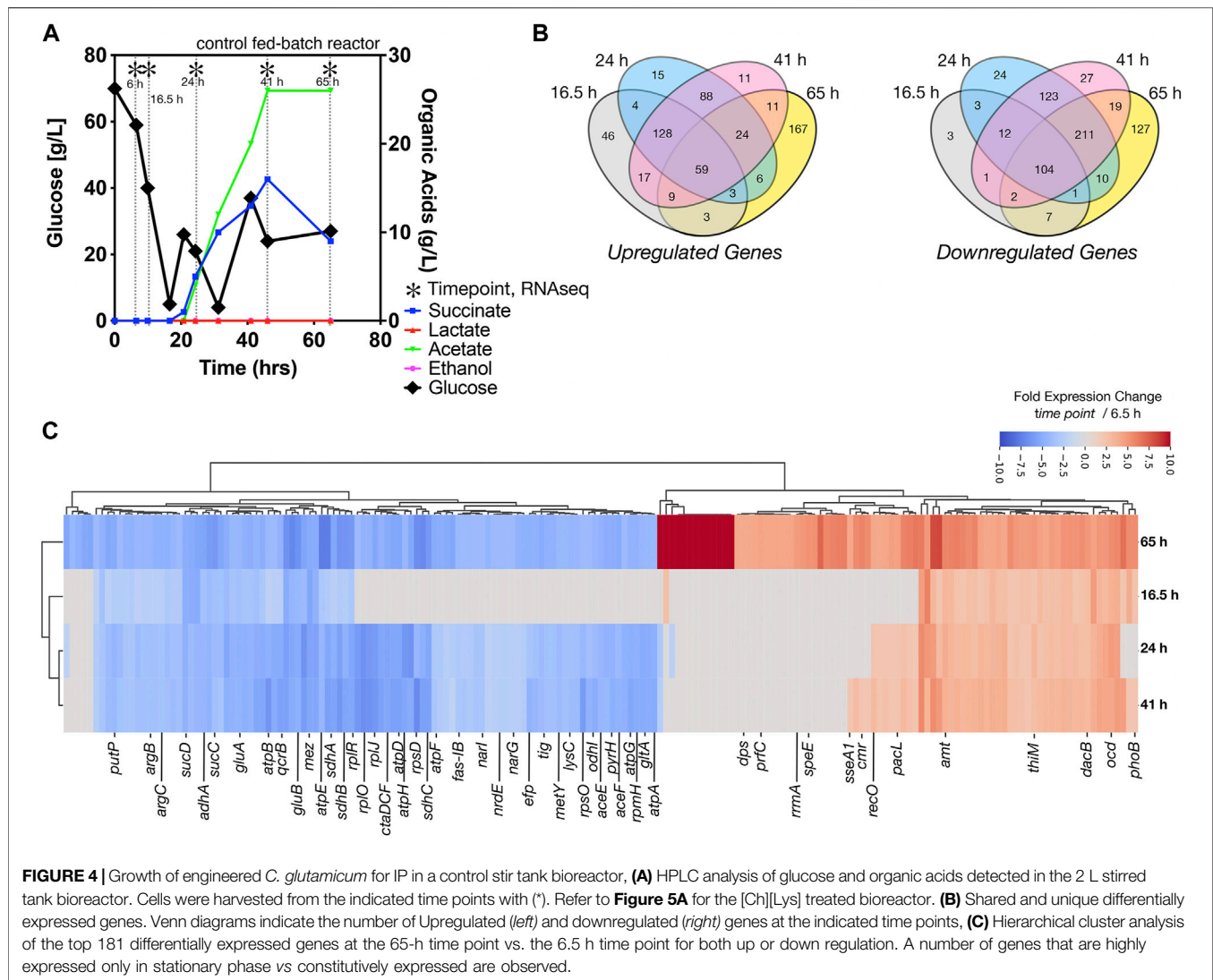
FIGURE 4 | Growth of engineered *C. glutamicum* for IP in a control stir tank bioreactor, **(A)** HPLC analysis of glucose and organic acids detected in the 2 L stirred tank bioreactor. Cells were harvested from the indicated time points with (*). Refer to **Figure 5A** for the [Ch][Lys] treated bioreactor. **(B)** Shared and unique differentially expressed genes. Venn diagrams indicate the number of Upregulated (*left*) and downregulated (*right*) genes at the indicated time points, **(C)** Hierarchical cluster analysis of the top 181 differentially expressed genes at the 65-h time point vs. the 6.5 h time point for both up or down regulation. A number of genes that are highly expressed only in stationary phase *vs* constitutively expressed are observed.

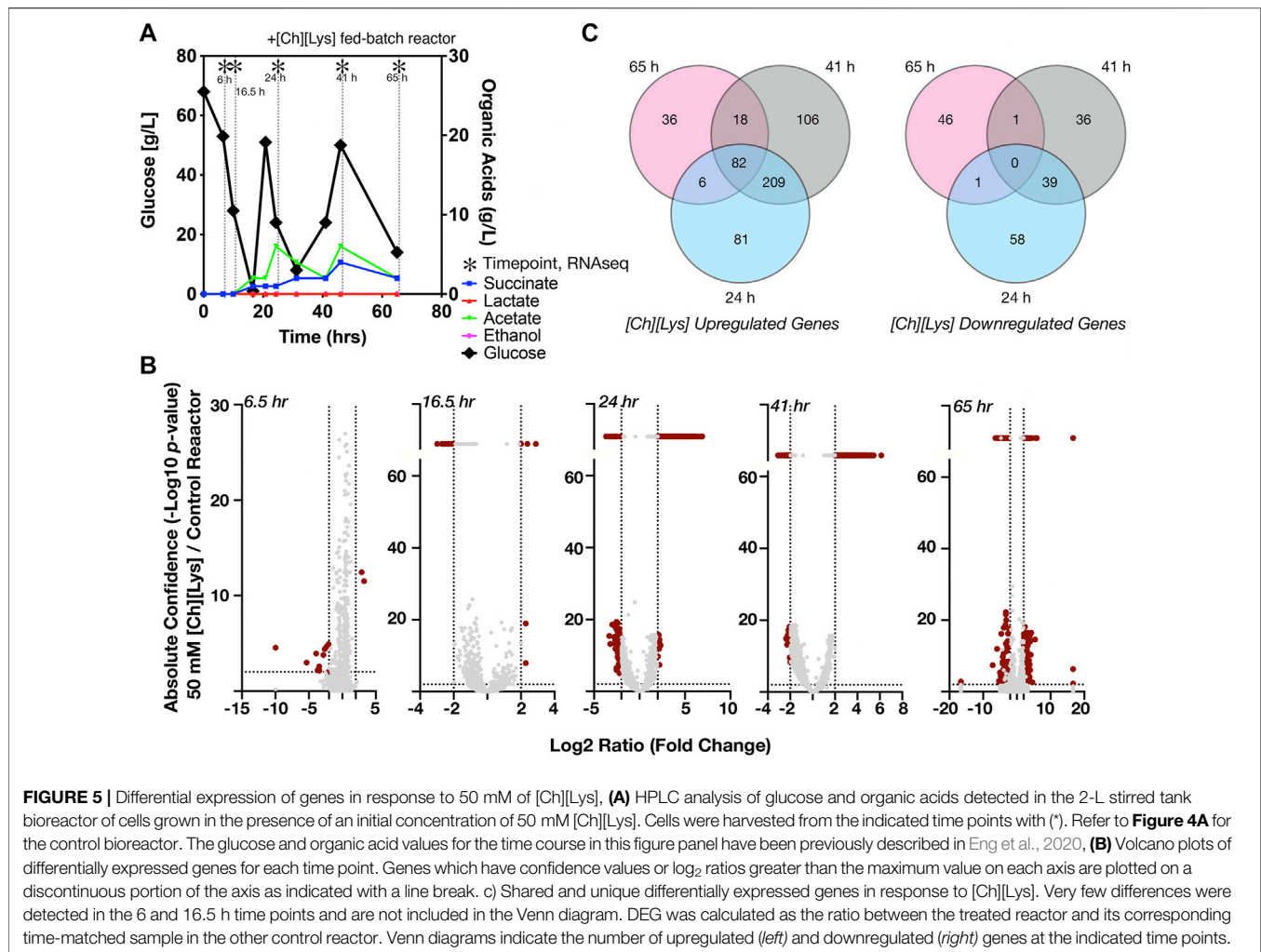*Escherichia coli* (Kang et al., 2019). Inositol is found in the yeast extract (>160 mg/g range) for many commercial preparations.

Overexpressed Regulatory and Stress Responsive Genes

A wide range of regulatory factors and stress responsive genes were also upregulated at the shake flask to bioreactor transition time point. Cgl2988/*malR*, which encodes for a MarR type transcriptional regulator and Cgl3007/*mez* were both highly upregulated. MalR represses expression of the malic enzyme gene, *mez* (Krause et al., 2012) and is a global regulator of stress-responsive cell envelope remodeling in *C. glutamicum* (Hünnefeld et al., 2019). Cgl2996/*ino-1* (myo-inositol-1-phosphate synthase) is the first enzyme in mycothiol biosynthesis and plays a major role in the detoxification of stress-inducing factors, maintaining the redox balance and protection against oxidative stress (Chen et al., 2019). The universal stress response protein Cgl1407/*uspA2* and HSP 60 family chaperonin, Cgl2716/*groEL* were also upregulated.

Underexpressed Metabolic, Transporter and Regulatory Genes

A similar number of genes were downregulated during the transition from shake flask to bioreactor (**Figure 3B**). Of the genes uniquely downregulated at 6.5 h, included Cgl1427/*cmk*, cytidyl kinase, Cgl2605/*bioD*, thioredoxin reductase. Cgl1427 has been reported to be crucial for maintaining triphosphate pools (ATP, CTP) under oxygen-limiting environments (Takeno et al., 2013) but it's downregulation implies these early time points are not oxygen-limited. Several genes involved in transport were also significantly downregulated with a cutoff threshold log$_2$ ratio less than −4. These included ABC transporter ATPase proteins Cgl1351, Cgl1546/*pacL* (cation specific) and Cgl1567 along with Cgl2222, a major facilitator superfamily (MFS) transporter. Downregulated genes Cgl0026-Cgl0029 have been reported to be Zur-binding sites that are involved in zinc homeostasis in *C. glutamicum* (Schröder et al., 2010). Other downregulated transporters included the lysine exporter Cgl1262/*lysE*, exporter systems for branched chain amino acid

FIGURE 5 | Differential expression of genes in response to 50 mM of [Ch][Lys], **(A)** HPLC analysis of glucose and organic acids detected in the 2-L stirred tank bioreactor of cells grown in the presence of an initial concentration of 50 mM [Ch][Lys]. Cells were harvested from the indicated time points with (*). Refer to **Figure 4A** for the control bioreactor. The glucose and organic acid values for the time course in this figure panel have been previously described in Eng et al., 2020, **(B)** Volcano plots of differentially expressed genes for each time point. Genes which have confidence values or log$_2$ ratios greater than the maximum value on each axis are plotted on a discontinuous portion of the axis as indicated with a line break. c) Shared and unique differentially expressed genes in response to [Ch][Lys]. Very few differences were detected in the 6 and 16.5 h time points and are not included in the Venn diagram. DEG was calculated as the ratio between the treated reactor and its corresponding time-matched sample in the other control reactor. Venn diagrams indicate the number of upregulated (*left*) and downregulated (*right*) genes at the indicated time points.

and methionine (*brnE/brnF*) along with several MFS transporters (Cgl1065, Cgl1076/*pcaK*, Cgl0380, Cgl0381, Cgl2685/*lmrB*) and the ABC type phosphate uptake system (*pstSCAB*). Several other ABC transporter subunits (permease or substrate-binding domain or the ATPase) responsible for transport of iron, calcium, cobalt, cadmium, copper, sn-glycerol-3-phosphate were also downregulated. Downregulated transcriptional regulators during this scale transition phase belong to the GntR family (Cgl2316), ArsR family (Cgl2279), PadR family (Cgl2979) and CopY family (Cgl0385). A complete list of DEGs can be found in **Supplementary Dataset S1 through S6** and at the JGI Genome Portal (https://genome.jgi.doe.gov/portal/) under Project ID 1203597.

Metabolic Pathway Alterations During Fed-Batch Cultivation Indicated by Differentially Expressed Genes

After inoculation into the bioreactors, we benchmarked the bioreactor run with online and offline measurements including growth, glucose consumption, and organic acid secretion, with and without [Ch][Lys]. We noted several differences between cells grown in the control reactor

and the [Ch][Lys] treated reactor. While cells were pulse-fed the same feed solution to restore glucose levels back to 60 g/L, the [Ch][Lys] treated engineered strain produced much less acetate and succinate than the control (**Figures 4A**, **5A**). Overall OD$_{600}$ measurements indicated similar initial growth patterns before the first feeding, but after feeding, OD$_{600}$ measurements did not appreciably increase further and instead we detected overflow metabolite accumulation above 10 g/L of succinate and acetate (**Figure 4A**). The control reactor decreased in OD$_{600}$ from a high of 49 to a 21 OD$_{600}$. The [Ch][Lys] reactor also decreased in OD$_{600}$, but from a similar high of 50 to 36 OD$_{600}$ (**Supplementary Figure S2**). We correlated gene expression changes during this campaign for both reactors using RNAseq analysis to understand how glucose was redirected from growth to the generation of these overflow metabolites (**Supplementary Dataset S2**).

Differentially Expressed Metabolic Genes

We observed several genes encoding metabolic processes related to succinate and acetate metabolism were downregulated in the time course, such as *ptaA, ackA* and *sucC*. Decreasing their gene expression suggests a decrease in activity, enabling greater succinate or acetate accumulation due to fewer competing reactions for these metabolites as precursors. Cgl2211, a putative

succinate exporter (Huhn et al., 2011; Litsanov et al., 2012; Prell et al., 2020) was upregulated at 65 h, that might explain higher succinate excretion profile for the fed-batch cultivation in the absence of the IL (**Figure 4A**). The higher acetate secretion in this bioreactor correlated with upregulated Cgl2066 transcripts at 24 and 41 h, which encodes a putative acyl phosphatase that converts acetyl phosphate to acetate. At the last phase of cultivation Cgl2380/*mdh* was upregulated (log$_2$ ratio of 3.14) with 12-fold over expression. Malate dehydrogenase, *mdh*, is involved in a NADH based reversible reaction in TCA and is responsible for NADH balance maintenance and succinate formation. The malic enzyme, Cgl3007/*mez,* was downregulated across all later time points (log$_2$ ratio of −3.1 to −7.65), with 10-fold decrease in expression in the last time point alone. Malic enzyme, upregulated during transition from shake flask to a bioreactor scale (log$_2$ ratio of 5.11 at 6.5 h), is involved in gluconeogenesis important for NADPH regeneration for anabolic processes and pyruvate flux at the cost of carbon loss as 1 mole of CO_2. The later time points (24 h and later) had many shared downregulated genes (211 genes), indicating a phenotypic similarity (**Figure 4B**). We also observed significant downregulation of *adhA*, *ald*, *sucCD*, *malE/mez* (**Figure 4C**, blue colored genes)*,* which were previously reported during microaerobic aeration in a bioreactor cultivation of *C. glutamicum* (Lange et al., 2018).

Differentially Expressed Transporter Genes

A more comprehensive analysis of differential gene expression indicated that many transporters were upregulated in these bioreactor time points (**Figure 4C**, red colored genes). These included ABC transporters for phosphonate (*pctABCD*); sn-glycerol-3-phosphate (*ugpABCE*) and phosphate (*pstSCAB),* a branched chain amino acid and methionine exporter (Cgl0258/*brnF*); Cgl0968/*lysI*, which encodes a protein involved in lysine uptake (Seep-Feldhaus et al., 1991). Cgl1502, a putative MFS transporter (PTS based sugar importer) was upregulated in all later bioreactor cultivation time points. A different complement of transport-related genes were also downregulated across all the later time points that included genes encoding for maltose and trehalose ABC transporter subunits (Cgl2460 and Cgl0727) and the entire glutamate ABC transporter operon *gluABCD*.

Overexpressed Regulatory Genes

Transcriptional regulators that were upregulated across all the later time points of the bioreactor cultivation and were associated with putative functions included Cgl2496/PucR family, Cgl0962/TetR family, Cgl2934/MarR family, Cgl1367/LacI family and Cgl2616/LysR family. Cgl2776 which is a putative XRE family transcriptional regulator MsrR was found to be upregulated from 24 to 65 h. *msrR* is located downstream of the *cmr* gene that encodes for a MFS multidrug efflux protein and upstream of Cgl2775/*sseA1*, a sulfurtransferase and Cgl2774. These late-phase upregulated genes have been previously reported to be regulated by MsrR and overexpressed in response to oxidative stress response in *C. glutamicum* (Si et al., 2020). Genes under the control of DtxR, a master regulator of iron homeostasis at late exponential phase (Küberl et al., 2020), and AmtR, a master regulator of nitrogen metabolism (Beckers et al., 2005) were also upregulated at later time

points compared to 6.5 h. The iron homeostasis genes included Cgl0387 (putative membrane protein) and Cgl2035, an ABC-type cobalamin/Fe^{3+}-siderophores transporter. The nitrogen metabolism regulon included genes encoding for ammonium permease, *amt*; a predicted ornithine decarboxylase (*ocd*) and the ABC transporter for urea UrtABCDE. Ammonium is a critical precursor for growth and tetramethylpyrazine (TMP) production (Xiao et al., 2014). A regulator involved in diverting acetyl CoA flux towards fatty acid biosynthesis, Cgl2490/*fasR* was constitutively expressed up until the last time point during bioreactor cultivation in absence of IL. This TetR type transcriptional regulator controls fatty acid biosynthesis and malonyl CoA formation from acetyl CoA and has been deleted for improving malonyl CoA production (Milke et al., 2019). Our analysis correlated this repression by *fasR* with down regulated Cgl2495/*fas-IA* as well as downregulation of Cgl0700/*accBC*, Cgl0708/*dtsR1* and Cgl0707/*dtsR2* during later time points in absence of IL.

Underexpressed Cell Division Genes

Genes encoding cell division proteins including *mraZ, ftsX, ftsW, ftsE, sepF,* were downregulated for later stage cultivation time points (24 h and later) correlating with the lack of increased OD$_{600}$ after glucose was fed at the 24-h time point.

Differentially Expressed Genes at Endpoint Bioreactor Cultivation

We observed a unique class of genes that were only expressed after high accumulation of succinate and acetate at the 65-h time point. At this time point, glucose consumption has stalled, and the overflow organic acids have plateaued at the ~10 g/L concentration. Genes encoding for ROS detoxification including catalase gene Cgl0255/*katA*, superoxide dismutase gene Cgl2927/*sod* along with Cgl2003/*gor,* a mycothione reductase involved in arsenate detoxification were upregulated. DEGs that were downregulated included genes encoding for *catA2, catC, nagI, qsuB, benC* and *benD*. These are enzymes involved in aromatic compound degradation through beta-ketoadipate pathway that would reroute flux into TCA through succinate and acetyl CoA.

Together the differential gene expression profile suggests that at the cell density reached by 20 h, there was a general cell stress response and the activation of microaerobic-specific genes. The growth conditions did not promote additional cell growth due to the downregulation of cell division genes; glucose uptake genes were still highly active, enabling a significant conversion of glucose to organic acids but not biomass accumulation. We interpret the expression of these genes as indicative of the unfavorable growth conditions.

C. glutamicum Exhibits a Complex Response to the IL, Cholinium Lysinate Under Fed-Batch Cultivation in the Bioreactor

Next we analyzed differential gene expression when cells were grown in the presence of 50 mM [Ch][Lys], simulating
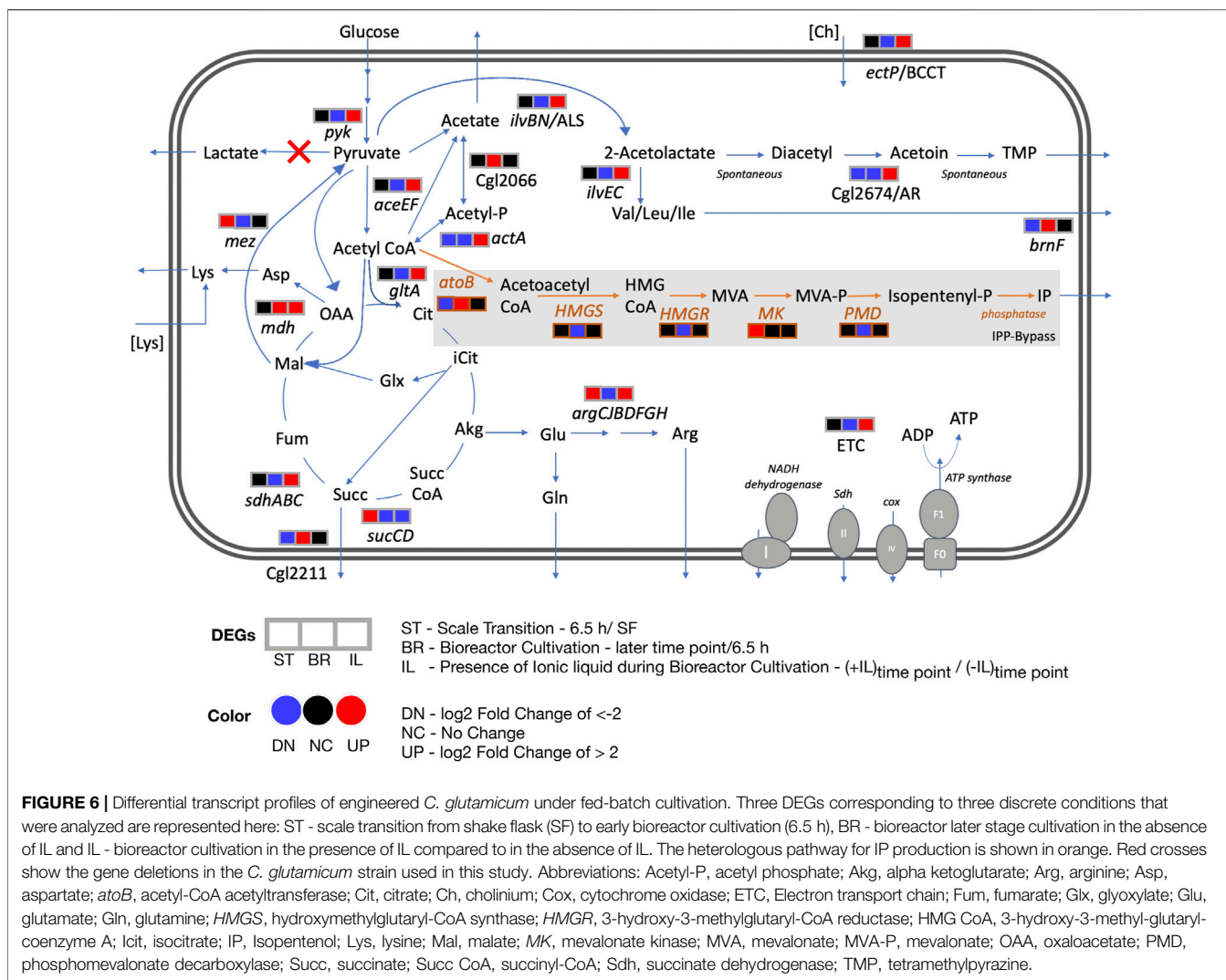
FIGURE 6 | Differential transcript profiles of engineered *C. glutamicum* under fed-batch cultivation. Three DEGs corresponding to three discrete conditions that were analyzed are represented here: ST - scale transition from shake flask (SF) to early bioreactor cultivation (6.5 h), BR - bioreactor later stage cultivation in the absence of IL and IL - bioreactor cultivation in the presence of IL compared to in the absence of IL. The heterologous pathway for IP production is shown in orange. Red crosses show the gene deletions in the *C. glutamicum* strain used in this study. Abbreviations: Acetyl-P, acetyl phosphate; Akg, alpha ketoglutarate; Arg, arginine; Asp, aspartate; *atoB*, acetyl-CoA acetyltransferase; Cit, citrate; Ch, cholinium; Cox, cytochrome oxidase; ETC, Electron transport chain; Fum, fumarate; Glx, glyoxylate; Glu, glutamate; Gln, glutamine; *HMGS*, hydroxymethylglutaryl-CoA synthase; *HMGR*, 3-hydroxy-3-methylglutaryl-CoA reductase; HMG CoA, 3-hydroxy-3-methyl-glutaryl-coenzyme A; Icit, isocitrate; IP, Isopentenol; Lys, lysine; Mal, malate; *MK*, mevalonate kinase; MVA, mevalonate; MVA-P, mevalonate; OAA, oxaloacetate; PMD, phosphomevalonate decarboxylase; Succ, succinate; Succ CoA, succinyl-CoA; Sdh, succinate dehydrogenase; TMP, tetramethylpyrazine.

hydrolysate prepared under a water-conservation regimen (Neupane et al., 2017). ILs have been reported to increase osmotic pressure, interact with lipid structures and consequently disrupt microbial membranes (Thuy Pham et al., 2010; Khudyakov et al., 2012; Yu et al., 2016). *C. glutamicum* exhibited differential expression of 727 genes (**Supplementary Dataset S3**), during the [Ch][Lys] treated fed-batch bioreactor cultivation in comparison to the untreated culture at the time-matched samples (**Figure 5A**). While both bioreactors consumed the initial glucose in the reactor at similar rates, their response to the first feeding at 24 h differed. The [Ch][Lys] reactor showed maximum accumulation of 4 g/L succinate and 6 g/L acetate over the duration of this time course, a 4-fold decrease for both organic acids in the absence of [Ch][Lys] (compare **Figures 4A**, **5A**). In the presence of [Ch][Lys], genes encoding for succinate utilization such as *sdhA*, *sdhB* and *sdhC* were all upregulated at 24 and 41 h in contrast to the control reactor. Similarly, genes encoding for pyruvate decarboxylation to acetyl CoA (instead of acetate) via *aceE* and *aceF* were also highly upregulated at later time points.

During the early cultivation time points (6.5–16.5 h), only 1.5% of the total pool of differentially expressed genes changed in response specifically to [Ch][Lys], but the datasets diverged after the first feeding at 24 h as biomass formation reached its maximum (**Figure 5B**). Only two genes were upregulated at the 6.5 h time point: a MFS transporter (Cgl2611) and its transcriptional regulator (Cgl2612) (**Supplementary Dataset S3**). The BRC-JBEI 1.1.2 homolog is 97.37% identical to Cgl2611 which exports cadaverine, a L-lysine derived product (Kind et al., 2011; Adkins et al., 2012; Jones et al., 2015; Tsuge et al., 2016). Cgl2611 expression was not detected at the control 6.5 h time point, but both genes are highly upregulated with or without [Ch][Lys] treatment in the remaining time points. Cgl1203, which encodes a phospho-N-acetylmuramoyl-pentapeptide-transferase associated with cell wall biosynthesis, was only upregulated at 16.5 h.

Early transcriptome changes in *C. glutamicum* during bioreactor cultivation post [Chl][Lys] exposure included overexpression of MFS transporters along with repression of mechanosensitive channels that were consistent with IL

tolerance mechanisms reported in other microbes (Khudyakov et al., 2012; Martins et al., 2013; Yu et al., 2016). Many genes were downregulated in response to exogenous [Ch][Lys] in the bioreactor and represented 25% of DEGs. Cgl0879/*mscL*, a large-conductance mechanosensitive channel, that is related to osmotic regulation (Krämer, 2009), was uniquely downregulated at 16.5 h.

A comprehensive analysis of upregulated DEGs at more than one time point represented around 59% of the total upregulated genes in the presence of IL (**Figure 5B**). Nearly 15% of those genes showed consistent overexpression from 24 h through 65 h (**Figure 5C**). This differential transcript profile reflects the metabolic perturbation over the course of the fed-batch cultivation after the initial glucose exhaustion followed by glucose pulse feeding and is depicted in **Figure 6**. Prominent DEGs include those encoding for energy metabolism, amino acids biosynthesis, response to oxidative and other environmental stress conditions (**Supplementary Dataset S4**).

Overexpressed Metabolic Genes

Genes involved in energy metabolism were highly upregulated during the later phase of fed-batch cultivation in the presence of IL compared to its absence. These included NADH dehydrogenase (Cgl1465), succinate dehydrogenase, *sdhABC* genes at 24 and 41 h; cytochrome oxidase, *ctaDCEF*, cytochrome reductase, *qcrCAB* and the ATP synthase complex (Cgl1206 to Cgl1213) genes at 24, 41 and 65 h. Amino acid biosynthetic genes upregulated at the later time points included the arginine biosynthetic genes *argC, argJ, argB* and *argH* at 65 h and *argG* and *argD* at mid cultivation phase (41 h). ArgJ protein was also enriched in the acetoin/TMP producing *C. glutamicum* strain (Eng et al., 2020). Genes encoding for other amino acid biosynthesis included Cgl1139/*metE*, Cgl2446/*metB* and Cgl0653/*metY* at 24 and 41 h from the methionine/homocysteine pathway; Cgl2204/*ilvE* at 24 h and Cgl1273/*ilvC* at 24 and 41 h in the branched amino acid pathway.

Overexpressed Genes Encoding Ribosomal Proteins

Several ribosomal proteins were significantly upregulated during the same cultivation phase (24 and 41 h) including 30S ribosomal proteins S15 (Cgl1976/*rpsO*) and S18 (Cgl0866/*rpsR*); 50S ribosomal proteins L28 (Cgl0869/*rpmB*) and L15 (Cgl0542/*rplO*) along with the ribosome recycling factor Cgl2023/*frr*.

Overexpressed Transporter Genes

We also observed the upregulation of an ABC transporter (Cgl0946 and Cgl0947), a multidrug transport system (MTS) operon, in part regulated by its adjacent two-component system (TCS) (Cgl0948-Cgl0949, also upregulated). MTS offers a natural defense against toxic compounds and is reported to be upregulated in response to the non-ionic surfactant Tween 40 (Jiang et al., 2020). Also, Cgl2312/*ectP*, a putative BCCT family transporter was overexpressed in the bioreactor with IL at 24 h time point. This gene, an orthologue for *betT* gene in *E. coli* and *P. putida*, was under-expressed in the bioreactor without IL at later time points (24 h, 41 h). Betaine/carnitine/choline (BCCT) family transporters could enable cholinium uptake and catabolism. An

array of other transporters and transcriptional regulators were also downregulated in the presence of IL (**Supplementary Dataset S3**).

While the analysis above compared matched time points with or without [Ch][Lys] treatment, we also included one additional analysis to examine DEGs from samples in the same reactor but as they progressed from the 41 to 65 h time point (**Supplementary Figure S3**, and **Supplementary Dataset S6**). As observed from our earlier analysis in **Figure 4C** a set of DEGs in the control bioreactor were detected, consistent with entry into the stationary phase. Significantly downregulated genes also included genes encoding for a stationary phase repressor protein/redox responsive transcription factor, *whiB*/Cgl0599 (Walter et al., 2020) and a branched chain amino acid transporter (Cgl2250) (Graf et al., 2019). Cgl2250 has been reported to be downregulated during the transition from exponential to stationary phase in *C. glutamicum* (Larisch et al., 2007).

Indication of Flux Rerouting in the Presence of IL Stress During Fed-Batch Bioreactor Cultivation

Our transcriptome analysis identified differential profiles for energy metabolism, amino acid biosynthesis and redox related genes as discussed in the previous section (**Figure 6**). Several genes encoding for metabolic reactions related to acetoin and TMP accumulation were specifically upregulated in the presence of 50 mM of [Ch][Lys] at the 24 h or 41 h time points (**Supplementary Dataset S3**, **Supplementary Figure S4**) when compared to the control samples at the same time points. Of the two subunits of the acetolactate synthase (ALS) *ilvB and ilvN*, the smaller regulatory subunit, Cgl1272/*ilvN* was upregulated in the presence of IL fed-batch cultivation when compared to the absence of IL at 24 h. Acetolactate synthase in *C. glutamicum* takes part in diverting pyruvate flux towards branched chain amino acids biosynthesis and acetoin biosynthesis and could be a precursor to TMP (Eng et al., 2020) (**Figure 5**). Although branched chain amino acid biosynthesis has been extensively researched for engineering branched chain alcohol (e.g. isobutanol) producing *C. glutamicum* strains (Hasegawa et al., 2020) the branched chain amino acid degradation towards isopentenol biosynthesis (through HMG-CoA) and TCA through acetyl CoA still remains to be fully investigated. The other proposed enzyme in TMP accumulation is the NADH consuming acetoin reductase (AR, Cgl2674) and was also significantly upregulated ($\log_2 > 4$) at 41 h in presence of 50 mM of [Ch][Lys] compared to fed-batch cultivation in the absence of IL at similar time points. Genes encoding mechanisms that divert pyruvate flux towards acetyl CoA (Cgl2248/*aceE* and Cgl2207/*aceF*) were also upregulated along with genes for pyruvate kinase (Cgl2089/*pyk*) and citrate synthase (Cgl0829/*gltA*).

DISCUSSION

C. glutamicum is a strong contender as a microbial chassis for IP production and is already used at commercial scales. To test IP production in stirred-tank bioreactors, we used process

optimizations empirically identified for high IP titers in *E. coli* (Kang et al., 2019). In *E. coli*, Kang et al. reported IP titers > 3 g/L in fed-batch mode production; in contrast, these process parameters led to much lower IP titers in *C. glutamicum*. It is possible that these optimizations were specific to *E. coli*; the impact of this IP production pathway in *C. glutamicum* upon shifting from batch mode to fed-batch mode in a stirred tank bioreactor may have resulted in a different host-specific metabolic response.

What parameters are important in selecting one microbial host over another? From a genetic tractability perspective, *C. glutamicum*'s biggest drawback *vs.* model microbes such as *E. coli* could arise from its reduced transformation efficiency, which was lower by 3–5 orders of magnitude (Chung et al., 1989; Inoue et al., 1990; Ruan et al., 2015). However, Baumgart and coworkers made an astute observation; by using a methylation deficient strain of *C. glutamicum*, one could both improve transformation efficiency as well as plasmid copy number (Baumgart et al., 2013). Improved pathway copy number (both genomically integrated or plasmid-borne) in *E. coli* had already been shown to dramatically improve heterologous isoprenoid titers (Goyal et al., 2018; Chatzivasileiou et al., 2019). With this premise we initially used a methylation deficient strain as our starting host. However, the methylation deficient strain only produced trace titers of IP, but a related strain produced both improved IP titers 20x or a co-product, tetra-methylpyrazine. Understanding the genetic differences in this isolate BRC-JBEI 1.1.2 was the major thrust of this study.

Leveraging strain isolate differences is already commonplace when analyzing natively expressed products, such as natural products from *Streptomyces* spp. or wine, beer, and baking in *Saccharomyces* spp. (Nepal and Wang, 2019; Gallone et al., 2016). In *E. coli*, the Hanahan cloning strain DH1 is the preferred strain for the production of many terpenes, but experimentally identified modifications are needed to translate port pathways to other *E. coli* isolates as with the case for limonene production in *E. coli* BL21 (DE3) (Tsuruta et al., 2009; Rolf et al., 2020). A potential explanation for DH1 being a more robust host may be due to its elevated number of ribosomes compared to strains DH10, BL21, or BW25113 (Cardinale et al., 2013), which may indirectly help with heterologous pathway protein expression. Our whole-genome sequencing analysis identified a large number of genetic differences in our engineered isopentenol producing *C. glutamicum* BRC-JBEI 1.1.2 isolate (many associated with metabolic functions) that are unaccounted for when using the reference *C. glutamicum* genome. Previously we used computationally driven maximum theoretical yields calculations for a product across several microbes to evaluate microbial potential for a specific product/substrate pair (Banerjee et al., 2020). However, the accuracy of such predictions relies on the metabolic reactions curated for the reference strain and are challenging to apply in isolates used with differences at the genomic or metabolic level (refer to IP titers in **Figure 1A**). Pan-genome assemblies and metabolic models can be applied to this situation (both for BRC-JBEI 1.1.2 and DH1) to more accurately account for these metabolic features (Monk et al., 2013; Norsigian et al., 2018).

For emerging processes using IL pretreated lignocellulosic biomass, *C. glutamicum* as the microbial IP producer for this process is compelling. To the best of our knowledge, this is the first transcriptomics analysis of an engineered isopentenol producing *C.*

glutamicum strain in fed-batch conditions. Due to the relative similarity between this isolate to the type strain, we were able to use existing gene annotations with a fairly low homology cutoff (> 70%) for the majority of detected transcripts in this study. A large number of significant DEGs identified in this analysis encode hypothetical proteins that lack functional information. These genes can be further characterized using functional genomics tools such as parallelized transposon mutant libraries (Lim et al., 2019; Cain et al., 2020) or high throughput transcription factor characterization (Rajeev et al., 2011; Rajeev et al., 2014) to improve our understanding of these useful *C. glutamicum* isolates.

Our analysis here indicated a number of actionable targets for future studies to improve isopentenol titers under stirred tank fed-batch conditions. Deleting *mdh* could limit accumulation of succinate, a highly overexpressed gene. Deleting or down regulating *gltA*, Cgl2211, *brnF* and arginine biosynthesis genes that were also highly upregulated (**Figure 6**); could enlarge the acetyl-CoA pool, in turn improving IP titers. Additional gene targets should include *pta-ackA*, *poxB*, *actA* and Cgl2066 to block acetate formation. These proposed targets are specific to *C. glutamicum* host engineering for isopentenol production. Our transcriptomics analysis also implicated *ectP*, a BCCT family transporter similar to *E. coli betT* and *P. putida betT-III*, as a transporter for [Ch][Lys]; *ectP* was overexpressed in the presence of ILs. A BCCT transporter has been proposed to be involved in uptake and catabolism of the cholinium ion from [Ch][Lys] in both *E. coli* and *P. putida* (Park et al., 2020). Characterizing IL tolerance is an active research thrust in our laboratory.

In summary, our transcriptomic analysis under industrially relevant process conditions provides a toehold for future DBTL cycles. Future learn steps can leverage the information gleaned here to target the critical features implicated for improved *C. glutamicum* strain performance when producing desirable products, like isopentenol. Even accounting for potential increased cell heterogeneity in the bioreactor (Wehrs et al., 2019), important features both common and unique to conditions allow a closer look into cell physiology.

MATERIALS AND METHODS

Reagents and Experimental Conditions

In a previous report (Sasaki et al., 2019), we referred to the IP producing *C. glutamicum* strain as ATCC 13032 NHRI 1.1.2, as indicated in our archival notes. As we cannot confirm the provenance of *C. glutamicum* BRC-JBEI 1.1.2 and how it may have been derived from its closest relatives *C. glutamicum* SCgG1 or SCgG2, we opted to give this strain a unique identifier to avoid further confusion.

Unless indicated elsewhere, all reagents used were molecular biology grade or higher. Primers were synthesized by IDT DNA Technologies (Coralville, IA). CGXII media was prepared as previously described (Sasaki et al., 2019; Keilhauer et al., 1993). All strains and plasmids used in this study are described in **Supplementary Table S2**. *C. glutamicum* strains were struck to single colonies from glycerol stock on LB plates containing the appropriate antibiotic and prepared for production runs as previously described (Eng et al., 2020). The fed-batch cultivation

with 50 mM of [Ch][Lys] supplementation was previously described in (Eng et al., 2020). The control bioreactor without [Ch][Lys] was conducted at the same time and the glucose feeding regime was identical to that of the ionic liquid (IL) supplemented reactor. For RNAseq extraction, 5 ml culture samples were harvested in 1 ml aliquots, collected by centrifugation at 14,000 × g for 3 min, and stored at −80°C until subsequent RNA extraction. The supernatant from one of the appropriate time point aliquots was processed for organic acid analysis as described previously (Eng et al., 2020). Lab-scale IP production in deep well plates or 5 ml culture tubes were conducted as previously described (Eng et al., 2020). Isopentenol titers reported for the deep well plate format were corrected for evaporation at the 48 h time point as conducted previously (Sasaki et al., 2019). Exogenous [Ch][Lys] toxicity against *C. glutamicum* ATCC13032 and BRC-JBEI 1.1.2 was analyzed in a 48-well microtiter dish format. Cells were first adapted two times in CGXII minimal media with 4% (w/v) D-glucose. When cells were back diluted into fresh media in the microtiter dish, the starting Optical Density (OD) was set to 0.1 with a fill volume of 200 μl. The plate was incubated with shaking at 30°C and exogenous [Ch][Lys] added at the start of the time course. OD was monitored at 600 nm on a Synergy 4 plate reader (BioTek Instruments, Winooski VT) with the continuous shaking setting.

Production Run With Ensiled Sorghum Hydrolysate

CGXII minimal media was supplemented with ensiled sorghum biomass hydrolysate to test the ability of *C. glutamicum* BRC-JBEI 1.1.2 to utilize carbon sources from renewable feedstock pretreated with IL. Briefly, the forage sorghum (NK300 type, grown in Fresno, CA) was planted in Spring 2020 and harvested in Fall 2020. A forage harvester was used to both harvest and chop the sorghum biomass, which was then loaded in a silage pit, inoculated, and covered to maintain anaerobic conditions. The pit was opened in November 2020 and a sample of the ensiled material was collected, packed with dry ice while in transit, and stored at 4°C. A 210 L scale Andritz Hastelloy C276 pressure reactor (AG, Graz, Austria) with a helical impeller was utilized to process ensiled sorghum for the pretreatment and saccharification processes. Ensiled sorghum biomass was pretreated at 20% w/w solid loading with 10% w/w [Ch][Lys] at 140°C for 3 h with a mixing speed of 30 rpm. Solid loading was calculated based on the dry matter content determined using a Binder VDL115 vacuum oven. After 3 h at the target temperature, the reactor was cooled to room temperature before proceeding with the next steps. The Andritz reactor is sealed during this process, preventing contamination until further processing. Following pretreatment, the pretreated materials were adjusted to pH 5.1 using 50% v/v sulfuric acid and an enzyme cocktail of Novozyme, Inc. Cellic Ctec3 and Cellic Htec3 commercial enzymes in a ratio of 9:1 was added. Concentration of the commercial stocks were determined using Bradford assays and bovine serum albumin as a reference. Enzyme load was conducted at a ratio of 10 mg enzyme per 1 g of dry weight biomass. Following pH adjustment and enzyme addition, RODI water was added to obtain a final solid loading of 18.70%. Saccharification by enzymatic hydrolysis was operated at 50°C, 30 rpm for 70 h (Barcelos et al., 2021). The hydrolysate was then sequentially filtered using a filter press

through 5, 1, and 0.25 μm filters. Final filter sterilization was completed with a 0.2 μm filter and stored at −80°C until further use. This hydrolysate was thawed and added in place of water in CGXII media (amounting to 2.8 % (w/v) glucose), pH was adjusted to 7.4 and filter sterilized one additional time before use. We make the assumption the hydrolysate contained no biologically available nitrogen. To maintain a C/N ratio of glucose/ammonium sulfate + urea of 2.8, pure glucose powder was supplemented to the hydrolysate CGXII cultivation medium composition (Sasaki et al., 2019).

DNA and RNA Isolation

Genomic DNA from *C. glutamicum* BRC-JBEI 1.1.2 was isolated with the following protocol. In brief, strains from glycerol stocks were struck to single colonies on LB plates grown at 30°C overnight. A single colony was then inoculated into a 250 ml shake flask with 25 ml LB media and grown overnight to saturation. Cells were collected by centrifugation at 4,000 × g for 5 min. The cell pellet was then resuspended in 2 ml lysis buffer (2 mM EDTA, 250 mM NaCl, 2% (w/v) SDS, 2% (v/v) Triton-X 100, 2% (v/v) Tween-80, 5 mM DTT, 30 units Zymolase 100T, 1 mg/ml RNaseA). Zymolyase was supplied by US Biological (Salem, MA). The cells were initially incubated at 50°C for 30 min to promote protease activity and then incubated for an additional 3 h at 37°C with occasional mixing, at which point the lysate became noticeably viscous. DNA was extracted following standard protocols for isolation of DNA using phenol chloroform: isoamyl alcohol and subsequent isopropanol precipitation (Sambrook and Russell, 2001).

RNA was extracted from *C. glutamicum* samples using a Direct-Zol RNA Kit (Zymo Research, Irvine, CA) following the manufacturer's protocol. *C. glutamicum* cells were lysed after initially resuspending the cell pellet in 500 μl TRI reagent and mixed with glass beads. This mixture was then subject to cell disruption using a bead-beater (Biospec Inc., Bartlesville, OK) with a 3-min homogenization time at maximum intensity. After bead beating, samples were collected following the manufacturer's protocol without any additional modifications. RNA quality was assessed using a BioAnalyzer (Agilent Technologies, Santa Clara, CA) before RNA library preparation and downstream analysis.

For 16S ribosomal sequencing, *C. glutamicum* ATCC 13032 Δmrr and *C. glutamicum* JBEI-BRC 1.1.2 were struck from glycerol stocks to single colonies on LB plates and incubated overnight at 30°C. A single colony was isolated and boiled in 50 μl dH$_2$0 for 10 min. 1 μl of the boiled colony was used for PCR with primer pair (JGI_27F: 5′-AGAGTTTGATCCTGGCTCAG-3′   and JGI_1391R: 5′-GACGGGCRGTGWGTRCA-3′) with NEB Q5 Polymerase (New England Biolabs, Ipswitch, MA). The PCR amplicon was confirmed by agarose gel electrophoresis and the sequence was determined using conventional Sanger Sequencing (Genewiz LLC, Chelmsford, MA).

PacBio Genome Assembly

DNA sequencing was generated at the DOE Joint Genome Institute (JGI) using the Pacific Biosciences (PacBio) sequencing technology. A Pacbio SMRTbell(tm) library was constructed and sequenced on the PacBio Sequel and PacBio RS II platforms, which generated 397,096 filtered subreads (1,418,602,725 subread bases) totaling

3,352,276 bp. The mean coverage for this genome was 432.21x. All general aspects of library construction and sequencing performed at the JGI can be found at http://www.jgi.doe.gov.

RNAseq Library Generation and Processing for Illumina NGS

Stranded RNAseq library(s) were created and quantified by qPCR. Sequencing was performed using an Illumina instrument (refer to **Supplementary Table S3** for specifics per library). Raw fastq file reads were filtered and trimmed using the JGI QC pipeline resulting in the filtered fastq file (*.filter-RNA.gz files). Using BBDuk (https://sourceforge.net/projects/bbmap/), raw reads were evaluated for artifact sequence by kmer matching (kmer = 25), allowing for 1 mismatch and detected artifacts which were trimmed from the 3′ end of the reads. RNA spike-in reads, PhiX reads and reads containing any Ns were removed. Quality trimming was performed using the phred trimming method set at Q6. Following trimming, reads that did not meet the length threshold of at least 50 bases were removed.

Filtered reads from each library were aligned to the reference genome using HISAT2 version 2.2.0 (Kim et al., 2015). Strand-specific coverage bigWig files were generated using deepTools v3.1 (Ramírez et al., 2014). Next, featureCounts (Liao et al., 2014) was used to generate the raw gene counts (counts.txt) file using gff3 annotations. Only primary hits assigned to the reverse strand were included in the raw gene counts (-s 2 -p --primary options). Raw gene counts were used to evaluate the level of correlation between biological replicates using Pearson's correlation and determine which replicates would be used in the DEG analysis (**Supplementary Figure S5**). In the heatmap view, the libraries were ordered as groups of replicates. The cells containing the correlations between replicates have a purple (or white) border around them. For fragments per kilobase of transcript per million fragments mapped (FPKM) and TPM, normalized gene counts refer to SRA reads (Data availability section). A sample legend and description of RNAseq libraries used in this paper is described in **Supplementary Table S3**.

Transcriptome Analysis

Global transcriptome response under various experiment conditions were measured using Geneious Prime 2021 (https://www.geneious.com). The normalized expression was calculated and the differentially expressed genes (DEGs) were filtered for absolute $\log_2$ ratio >2 (i.e. a 4-fold up or down regulation), absolute confidence >3 ($p < 0.001$) and >90% sequence identity. The DEGs at various conditions were functionally annotated using Blast2GO suite (Götz et al., 2008) to assign GO annotations (Galperin et al., 2015). Each DEG was subjected to pathway analysis using the KEGG (Kyoto Encyclopedia of Genes and Genomes) database (http://www.kegg.jp/kegg/pathway.html) to explore the biological implications. Biocyc (https://biocyc.org/) was used to calculate pathway enrichment for the last 65 h/41 h time point and for additional gene orthologs identification. Pathways were considered significant if $p < 0.05$. Hierarchically clustered heat maps were generated with average linkage method and euclidean distance metric in Jupyter notebook using Python library Seaborn 0.11.1 (Waskom et al., 2020).

DATA AVAILABILITY STATEMENT

The datasets presented in this study can be found in online repositories. The names of the repository/repositories and accession number(s) can be found below: https://www.ncbi.nlm.nih.gov/, PRJNA533344 https://www.ncbi.nlm.nih.gov/, GCA_011761195.1 https://www.ncbi.nlm.nih.gov/, SRP23996 https://www.ncbi.nlm.nih.gov/, SRP239973 https://www.ncbi.nlm.nih.gov/, SRP239963 https://www.ncbi.nlm.nih.gov/, SRP239971 https://www.ncbi.nlm.nih.gov/, SRP239972 https://www.ncbi.nlm.nih.gov/, SRP239970 https://www.ncbi.nlm.nih.gov/, SRP2399a68 https://www.ncbi.nlm.nih.gov/, SRP239969 https://www.ncbi.nlm.nih.gov/, SRP239966 https://www.ncbi.nlm.nih.gov/, SRP239967 https://www.ncbi.nlm.nih.gov/, SRP239964 https://www.ncbi.nlm.nih.gov/, SRP239965.

AUTHOR CONTRIBUTIONS

Raised Funds: AM and BS. Conceptualization of the project: AM and TE. Strain construction, molecular biology, bioreactor sample collection and processing: YS, TE, RH, and JT. Analytical Chemistry, IP Production Assays, IL toxicity assays: YS, TE, and AS. Interpreted results: YS, DB, TE, and AM. Contributed critical reagents: NS, AO, CS, DP, TE, YS, JT, and BS. RNAseq library generation, data collection, validation: VS, YS, and TE. Drafted the manuscript: DB, TE, and AM. All authors read, contributed feedback, and approved the final manuscript for publication.

SUPPLEMENTARY MATERIAL

The Supplementary Material for this article can be found online at: https://www.frontiersin.org/articles/10.3389/fbioe.2021.766674/full#supplementary-material

REFERENCES

Adkins, J., Pugh, S., McKenna, R., and Nielsen, D. R. (2012). Engineering Microbial Chemical Factories to Produce Renewable "Biomonomers". *Front. Microbio.* 3, 313. doi:10.3389/fmicb.2012.00313

Ashburner, M., Ball, C. A., Blake, J. A., Botstein, D., Butler, H., Cherry, J. M., et al. (2000). Gene Ontology: Tool for the Unification of Biology. *Nat. Genet.* 25, 25–29. doi:10.1038/75556

Banerjee, D., Eng, T., Lau, A. K., Sasaki, Y., Wang, B., Chen, Y., et al. (2020). Genome-scale Metabolic Rewiring Improves Titers Rates and Yields of the Non-native Product Indigoidine at Scale. *Nat. Commun.* 11, 5385. doi:10.1038/s41467-020-19171-4

Baral, N. R., Yang, M., Harvey, B. G., Simmons, B. A., Mukhopadhyay, A., Lee, T. S., et al. (2021). Production Cost and Carbon Footprint of Biomass-Derived Dimethylcyclooctane as a High Performance Jet Fuel Blendstock. *ACS Sustainable Chem. Eng.* 9, 11872–11882. doi:10.1021/acssuschemeng.1c03772

Barcelos, C. A., Oka, A. M., Yan, J., Das, L., Achinivu, E. C., Magurudeniya, H., et al. (2021). High-Efficiency Conversion of Ionic Liquid-Pretreated Woody Biomass to Ethanol at the Pilot Scale. *ACS Sustain. Chem. Eng.* 9, 4042–4053. doi:10.1021/acssuschemeng.0c07920

Baumgart, M., Unthan, S., Rückert, C., Sivalingam, J., Grünberger, A., Kalinowski, J., et al. (2013). Construction of a Prophage-free Variant of *Corynebacterium glutamicum* ATCC 13032 for Use as a Platform Strain for Basic Research and Industrial Biotechnology. *Appl. Environ. Microbiol.* 79, 6006–6015. doi:10.1128/AEM.01634-13

Becker, J., Rohles, C. M., and Wittmann, C. (2018). Metabolically Engineered *Corynebacterium glutamicum* for Bio-Based Production of Chemicals, Fuels, Materials, and Healthcare Products. *Metab. Eng.* 50, 122–141. doi:10.1016/j.ymben.2018.07.008

Beckers, G., Strösser, J., Hildebrandt, U., Kalinowski, J., Farwick, M., Krämer, R., et al. (2005). Regulation of AmtR-Controlled Gene Expression in *Corynebacterium glutamicum*: Mechanism and Characterization of the AmtR Regulon. *Mol. Microbiol.* 58, 580–595. doi:10.1111/j.1365-2958.2005.04855.x

Cain, A. K., Barquist, L., Goodman, A. L., Paulsen, I. T., Parkhill, J., and van Opijnen, T. (2020). A Decade of Advances in Transposon-Insertion Sequencing. *Nat. Rev. Genet.* 21, 526–540. doi:10.1038/s41576-020-0244-x

Cardinale, S., Joachimiak, M. P., and Arkin, A. P. (2013). Effects of Genetic Variation on the *E. coli* Host-Circuit Interface. *Cel Rep.* 4, 231–237. doi:10.1016/j.celrep.2013.06.023

Chatzivasileiou, A. O., Ward, V., Edgar, S. M., and Stephanopoulos, G. (2019). Two-step Pathway for Isoprenoid Synthesis. *Proc. Natl. Acad. Sci. USA.* 116, 506–511. doi:10.1073/pnas.1812935116

Chen, C., Chen, K., Su, T., Zhang, B., Li, G., and Pan, J. (2019). Myo-inositol-1-phosphate Synthase (Ino-1) Functions as a Protection Mechanism in *Corynebacterium glutamicum* Under Oxidative Stress. *Microbiologyopen.* 8, e00721. doi:10.1002/mbo3.721

Chou, H. H., and Keasling, J. D. (2012). Synthetic Pathway for Production of Five-Carbon Alcohols from Isopentenyl Diphosphate. *Appl. Environ. Microbiol.* 78, 7849–7855. doi:10.1128/AEM.01175-12

Chung, C. T., Niemela, S. L., and Miller, R. H. (1989). One-step Preparation of Competent *Escherichia coli*: Transformation and Storage of Bacterial Cells in the Same Solution. *Proc. Natl. Acad. Sci.* 86, 2172–2175. doi:10.1073/pnas.86.7.2172

Eng, T., Demling, P., Herbert, R. A., Chen, Y., Benites, V., Martin, J., et al. (2018). Restoration of Biofuel Production Levels and Increased Tolerance under Ionic Liquid Stress Is Enabled by a Mutation in the Essential *Escherichia coli* Gene cydC. *Microb. Cel Fact.* 17, 159. doi:10.1186/s12934-018-1006-8

Eng, T., Sasaki, Y., Herbert, R. A., Lau, A., Trinh, J., Chen, Y., et al. (2020). Production of Tetra-Methylpyrazine Using Engineered *Corynebacterium glutamicum*. *Metab. Eng. Commun.* 10, e00115. doi:10.1016/j.mec.2019.e00115

Gallone, B., Steensels, J., Prahl, T., Soriaga, L., Saels, V., Herrera-Malaver, B., et al. (2016). Domestication and Divergence of *Saccharomyces cerevisiae* Beer Yeasts. *Cell* 166, 1397–1410. doi:10.1016/j.cell.2016.08.020

Galperin, M. Y., Makarova, K. S., Wolf, Y. I., and Koonin, E. V. (2015). Expanded Microbial Genome Coverage and Improved Protein Family Annotation in the COG Database. *Nucleic Acids Res.* 43, D261–D269. doi:10.1093/nar/gku1223

Götz, S., García-Gómez, J. M., Terol, J., Williams, T. D., Nagaraj, S. H., Nueda, M. J., et al. (2008). High-throughput Functional Annotation and Data Mining with the Blast2GO Suite. *Nucleic Acids Res.* 36, 3420–3435. doi:10.1093/nar/gkn176

Goyal, G., Costello, Z., Alonso-Gutierrez, J., Kang, A., Lee, T. S., Garcia Martin, H., et al. (2018). Parallel Integration and Chromosomal Expansion of Metabolic Pathways. *ACS Synth. Biol.* 7, 2566–2576. doi:10.1021/acssynbio.8b00243

Graf, M., Haas, T., Müller, F., Buchmann, A., Harm-Bekbenbetova, J., Freund, A., et al. (2019). Continuous Adaptive Evolution of a Fast-Growing *Corynebacterium glutamicum* Strain Independent of Protocatechuate. *Front. Microbiol.* 10, 1648. doi:10.3389/fmicb.2019.01648

Hahne, J., Kloster, T., Rathmann, S., Weber, M., and Lipski, A. (2018). Isolation and Characterization of Corynebacterium Spp. From Bulk Tank Raw Cow's Milk of Different Dairy Farms in Germany. *PLoS ONE* 13, e0194365. doi:10.1371/journal.pone.0194365

Hasegawa, S., Jojima, T., Suda, M., and Inui, M. (2020). Isobutanol Production in *Corynebacterium glutamicum*: Suppressed Succinate By-Production by pckA Inactivation and Enhanced Productivity via the Entner-Doudoroff Pathway. *Metab. Eng.* 59, 24–35. doi:10.1016/j.ymben.2020.01.004

Hou, X.-D., Liu, Q.-P., Smith, T. J., Li, N., and Zong, M.-H. (2013). Evaluation of Toxicity and Biodegradability of Cholinium Amino Acids Ionic Liquids. *PLoS ONE* 8, e59145. doi:10.1371/journal.pone.0059145

Huhn, S., Jolkver, E., Krämer, R., and Marin, K. (2011). Identification of the Membrane Protein SucE and its Role in Succinate Transport in *Corynebacterium glutamicum*. *Appl. Microbiol. Biotechnol.* 89, 327–335. doi:10.1007/s00253-010-2855-1

Hünnefeld, M., Persicke, M., Kalinowski, J., and Frunzke, J. (2019). The MarR-type Regulator MalR Is Involved in Stress-Responsive Cell Envelope Remodeling in *Corynebacterium glutamicum*. *Front. Microbiol.* 10, 1039. doi:10.3389/fmicb.2019.01039

Inoue, H., Nojima, H., and Okayama, H. (1990). High Efficiency Transformation of *Escherichia coli* with Plasmids. *Gene* 96, 23–28. doi:10.1016/0378-1119(90)90336-P

Jiang, Y., Huang, M.-Z., Chen, X.-L., and Zhang, B. (2020). Proteome Analysis Guided Genetic Engineering of *Corynebacterium glutamicum* S9114 for Tween 40-triggered Improvement in L-Ornithine Production. *Microb. Cel Fact.* 19, 2. doi:10.1186/s12934-019-1272-0

Johnson, J. S., Spakowicz, D. J., Hong, B.-Y., Petersen, L. M., Demkowicz, P., Chen, L., et al. (2019). Evaluation of 16S rRNA Gene Sequencing for Species and Strain-Level Microbiome Analysis. *Nat. Commun.* 10, 5029. doi:10.1038/s41467-019-13036-1

Jones, C. M., Hernández Lozada, N. J., and Pfleger, B. F. (2015). Efflux Systems in Bacteria and Their Metabolic Engineering Applications. *Appl. Microbiol. Biotechnol.* 99, 9381–9393. doi:10.1007/s00253-015-6963-9

Kang, A., Mendez-Perez, D., Goh, E.-B., Baidoo, E. E. K., Benites, V. T., Beller, H. R., et al. (2019). Optimization of the IPP-Bypass Mevalonate Pathway and Fed-Batch Fermentation for the Production of Isoprenol in *Escherichia coli*. *Metab. Eng.* 56, 85–96. doi:10.1016/j.ymben.2019.09.003

Keilhauer, C., Eggeling, L., and Sahm, H. (1993). Isoleucine Synthesis in *Corynebacterium glutamicum*: Molecular Analysis of the ilvB-ilvN-ilvC Operon. *J. Bacteriol.* 175, 5595–5603. doi:10.1128/jb.175.17.5595-5603.1993

Khudyakov, J. I., D'haeseleer, P., Borglin, S. E., Deangelis, K. M., Woo, H., Lindquist, E. A., et al. (2012). Global Transcriptome Response to Ionic Liquid by a Tropical Rain forest Soil Bacterium, Enterobacter Lignolyticus. *Proc. Natl. Acad. Sci.* 109, E2173–E2182. doi:10.1073/pnas.1112750109

Kim, D., Langmead, B., and Salzberg, S. L. (2015). HISAT: a Fast Spliced Aligner with Low Memory Requirements. *Nat. Methods* 12, 357–360. doi:10.1038/nmeth.3317

Kind, S., Kreye, S., and Wittmann, C. (2011). Metabolic Engineering of Cellular Transport for Overproduction of the Platform Chemical 1,5-diaminopentane in *Corynebacterium glutamicum*. *Metab. Eng.* 13, 617–627. doi:10.1016/j.ymben.2011.07.006

Kinoshita, S., Nakayama, K., and Akita, S. (1958). Taxonomical Study of Glutamic Acid Accumulating Bacteria, Micrococcus Glutamicus Nov. Sp. *Bull. Agric. Chem. Soc. Jpn.* 22, 176–185. doi:10.1271/bbb1924.22.176

Koren, S., and Phillippy, A. M. (2015). One Chromosome, One Contig: Complete Microbial Genomes from Long-Read Sequencing and Assembly. *Curr. Opin. Microbiol.* 23, 110–120. doi:10.1016/j.mib.2014.11.014

Krämer, R. (2009). Osmosensing and Osmosignaling in *Corynebacterium glutamicum*. *Amino Acids* 37, 487–497. doi:10.1007/s00726-009-0271-6

Krause, J. P., Polen, T., Youn, J.-W., Emer, D., Eikmanns, B. J., and Wendisch, V. F. (2012). Regulation of the Malic Enzyme Gene malE by the Transcriptional Regulator MalR in *Corynebacterium glutamicum*. *J. Biotechnol.* 159, 204–215. doi:10.1016/j.jbiotec.2012.01.003

Küberl, A., Mengus-Kaya, A., Polen, T., and Bott, M. (2020). The Iron Deficiency Response of *Corynebacterium glutamicum* and a Link to Thiamine Biosynthesis. *Appl. Environ. Microbiol.* 86, 1–16. doi:10.1128/AEM.00065-20

Lange, J., Münch, E., Müller, J., Busche, T., Kalinowski, J., Takors, R., et al. (2018). Deciphering the Adaptation of *Corynebacterium glutamicum* in Transition from Aerobiosis via Microaerobiosis to Anaerobiosis. *Genes* 9, 297. doi:10.3390/genes9060297

Larisch, C., Nakunst, D., Hüser, A. T., Tauch, A., and Kalinowski, J. (2007). The Alternative Sigma Factor SigB of *Corynebacterium glutamicum* Modulates Global Gene Expression during Transition from Exponential Growth to Stationary Phase. *BMC Genomics* 8, 4. doi:10.1186/1471-2164-8-4

Liao, Y., Smyth, G. K., and Shi, W. (2014). featureCounts: an Efficient General Purpose Program for Assigning Sequence Reads to Genomic Features. *Bioinformatics* 30, 923–930. doi:10.1093/bioinformatics/btt656

Lim, H. C., Sher, J. W., Rodriguez-Rivera, F. P., Fumeaux, C., Bertozzi, C. R., and Bernhardt, T. G. (2019). Identification of New Components of the RipC-FtsEX Cell Separation Pathway of Corynebacterineae. *Plos Genet.* 15, e1008284. doi:10.1371/journal.pgen.1008284

Litsanov, B., Brocker, M., and Bott, M. (2012). Toward Homosuccinate Fermentation: Metabolic Engineering of *Corynebacterium glutamicum* for Anaerobic Production of Succinate from Glucose and Formate. *Appl. Environ. Microbiol.* 78, 3325–3337. doi:10.1128/AEM.07790-11

Magurudeniya, H. D., Baral, N. R., Rodriguez, A., Scown, C. D., Dahlberg, J., Putnam, D., et al. (2021). Use of Ensiled Biomass Sorghum Increases Ionic Liquid Pretreatment Efficiency and Reduces Biofuel Production Cost and Carbon Footprint. *Green. Chem.* 23, 3127–3140. doi:10.1039/D0GC03260C

Martins, I., Hartmann, D. O., Alves, P. C., Planchon, S., Renaut, J., Leitão, M. C., et al. (2013). Proteomic Alterations Induced by Ionic Liquids in Aspergillus nidulans and Neurospora Crassa. *J. Proteomics* 94, 262–278. doi:10.1016/j.jprot.2013.09.015

Milke, L., Kallscheuer, N., Kappelmann, J., and Marienhagen, J. (2019). Tailoring *Corynebacterium glutamicum* towards Increased Malonyl-CoA Availability for Efficient Synthesis of the Plant Pentaketide Noreugenin. *Microb. Cel Fact.* 18, 71. doi:10.1186/s12934-019-1117-x

Monk, J. M., Charusanti, P., Aziz, R. K., Lerman, J. A., Premyodhin, N., Orth, J. D., et al. (2013). Genome-scale Metabolic Reconstructions of Multiple *Escherichia coli* Strains Highlight Strain-specific Adaptations to Nutritional Environments. *Proc. Natl. Acad. Sci.* 110, 20338–20343. doi:10.1073/pnas.1307797110

Nepal, K. K., and Wang, G. (2019). Streptomycetes: Surrogate Hosts for the Genetic Manipulation of Biosynthetic Gene Clusters and Production of Natural Products. *Biotechnol. Adv.* 37, 1–20. doi:10.1016/j.biotechadv.2018.10.003

Neupane, B., Murthy Konda, N. V. S. N., Singh, S., Simmons, B. A., and Scown, C. D. (2017). Life-Cycle Greenhouse Gas and Water Intensity of Cellulosic Biofuel Production Using Cholinium Lysinate Ionic Liquid Pretreatment. *ACS Sustain. Chem. Eng.* 5, 10176–10185. doi:10.1021/acssuschemeng.7b02116

Norsigian, C. J., Kavvas, E., Seif, Y., Palsson, B. O., and Monk, J. M. (2018). iCN718, an Updated and Improved Genome-Scale Metabolic Network Reconstruction of Acinetobacter Baumannii AYE. *Front. Genet.* 9, 121. doi:10.3389/fgene.2018.00121

Opgenorth, P., Costello, Z., Okada, T., Goyal, G., Chen, Y., Gin, J., et al. (2019). Lessons from Two Design-Build-Test-Learn Cycles of Dodecanol Production in *Escherichia coli* Aided by Machine Learning. *ACS Synth. Biol.* 8, 1337–1351. doi:10.1021/acssynbio.9b00020

Park, M. R., Chen, Y., Thompson, M., Benites, V. T., Fong, B., Petzold, C. J., et al. (2020). Response of Pseudomonas Putida to Complex, Aromatic-Rich Fractions from Biomass. *ChemSusChem* 13, 4455–4467. doi:10.1002/cssc.202000268

Pérez-García, F., and Wendisch, V. F. (2018). Transport and Metabolic Engineering of the Cell Factory *Corynebacterium glutamicum*. *FEMS Microbiol. Lett.* 365, 1–11. doi:10.1093/femsle/fny166

Prell, C., Burgardt, A., Meyer, F., and Wendisch, V. F. (2020). Fermentative Production of L-2-Hydroxyglutarate by Engineered *Corynebacterium glutamicum* via Pathway Extension of L-Lysine Biosynthesis. *Front. Bioeng. Biotechnol.* 8, 630476. doi:10.3389/fbioe.2020.630476

Rajeev, L., Luning, E. G., Dehal, P. S., Price, M. N., Arkin, A. P., and Mukhopadhyay, A. (2011). Systematic Mapping of Two Component Response Regulators to Gene Targets in a Model Sulfate Reducing Bacterium. *Genome Biol.* 12, R99. doi:10.1186/gb-2011-12-10-r99

Rajeev, L., Luning, E. G., and Mukhopadhyay, A. (2014). DNA-affinity-purified Chip (DAP-Chip) Method to Determine Gene Targets for Bacterial Two Component Regulatory Systems. *J. Vis. Exp.* (89), 1–12. doi:10.3791/51715

Ramírez, F., Dündar, F., Diehl, S., Grüning, B. A., and Manke, T. (2014). deepTools: a Flexible Platform for Exploring Deep-Sequencing Data. *Nucleic Acids Res.* 42, W187–W191. doi:10.1093/nar/gku365

Reninger, N. S., and McPhee, D. J. (2008). Fuel Compositions Comprising Farnesane and Farnesane Derivatives and Method of Making and Using Same. Available at: https://patents.google.com/patent/US20080083158A1/en (Accessed August 14, 2021).

Rolf, J., Julsing, M. K., Rosenthal, K., and Lütz, S. (2020). A Gram-Scale Limonene Production Process with Engineered *Escherichia coli*. *Molecules* 25, 1881. doi:10.3390/molecules25081881

Ruan, Y., Zhu, L., and Li, Q. (2015). Improving the Electro-Transformation Efficiency of *Corynebacterium glutamicum* by Weakening its Cell wall and Increasing the Cytoplasmic Membrane Fluidity. *Biotechnol. Lett.* 37, 2445–2452. doi:10.1007/s10529-015-1934-x

Sabat, A. J., van Zanten, E., Akkerboom, V., Wisselink, G., van Slochteren, K., de Boer, R. F., et al. (2017). Targeted Next-Generation Sequencing of the 16S-23S rRNA Region for Culture-independent Bacterial Identification - Increased Discrimination of Closely Related Species. *Sci. Rep.* 7, 3434. doi:10.1038/s41598-017-03458-6

Sambrook, J., and Russell, D. Wi. (2001). *Molecular Cloning: A Laboratory Manual3 Volume Set)Cold Spring Harbor*. Third Edition (N.Y: Cold Spring Harbor Laboratory Press).

Santos, A. G., Ribeiro, B. D., Alviano, D. S., and Coelho, M. A. Z. (2014). Toxicity of Ionic Liquids toward Microorganisms Interesting to the Food Industry. *RSC Adv.* 4, 37157–37163. doi:10.1039/C4RA05295A

Sasaki, Y., Eng, T., Herbert, R. A., Trinh, J., Chen, Y., Rodriguez, A., et al. (2019). Engineering *Corynebacterium glutamicum* to Produce the Biogasoline Isopentenol from Plant Biomass Hydrolysates. *Biotechnol. Biofuels* 12, 41. doi:10.1186/s13068-019-1381-3

Schäfer, A., Tauch, A., Droste, N., Pühler, A., and Kalinowski, J. (1997). The *Corynebacterium glutamicum* cglIM Gene Encoding a 5-cytosine Methyltransferase Enzyme Confers a Specific DNA Methylation Pattern in an McrBC-Deficient *Escherichia coli* Strain. *Gene* 203, 95–101. doi:10.1016/S0378-1119(97)00519-2

Schröder, J., Jochmann, N., Rodionov, D. A., and Tauch, A. (2010). The Zur Regulon of *Corynebacterium glutamicum* ATCC 13032. *BMC Genomics* 11, 12. doi:10.1186/1471-2164-11-12

Seep-Feldhaus, A. H., Kalinowski, J., and Pühler, A. (1991). Molecular Analysis of the *Corynebacterium glutamicum* Gene Involved in Lysine Uptake. *Mol. Microbiol.* 5, 2995–3005. doi:10.1111/j.1365-2958.1991.tb01859.x

Si, M., Chen, C., Zhong, J., Li, X., Liu, Y., Su, T., et al. (2020). MsrR Is a Thiol-Based Oxidation-Sensing Regulator of the XRE Family that Modulates C. Glutamicum Oxidative Stress Resistance. *Microb. Cel Fact.* 19, 189. doi:10.1186/s12934-020-01444-8

Takeno, S., Shirakura, D., Tsukamoto, N., Mitsuhashi, S., and Ikeda, M. (2013). Significance of the Cgl1427 Gene Encoding Cytidylate Kinase in Microaerobic Growth of *Corynebacterium glutamicum*. *Appl. Microbiol. Biotechnol.* 97, 1259–1267. doi:10.1007/s00253-012-4275-x

Thuy Pham, T. P., Cho, C.-W., and Yun, Y.-S. (2010). Environmental Fate and Toxicity of Ionic Liquids: a Review. *Water Res.* 44, 352–372. doi:10.1016/j.watres.2009.09.030

Tsuge, Y., Kawaguchi, H., Sasaki, K., and Kondo, A. (2016). Engineering Cell Factories for Producing Building Block Chemicals for Bio-Polymer Synthesis. *Microb. Cel Fact.* 15, 19. doi:10.1186/s12934-016-0411-0

Tsuruta, H., Paddon, C. J., Eng, D., Lenihan, J. R., Horning, T., Anthony, L. C., et al. (2009). High-level Production of Amorpha-4,11-Diene, a Precursor of the Antimalarial Agent Artemisinin, in *Escherichia coli*. *PLoS ONE* 4, e4489. doi:10.1371/journal.pone.0004489

Walter, T., Veldmann, K. H., Götker, S., Busche, T., Rückert, C., Kashkooli, A. B., et al. (2020). Physiological Response of *Corynebacterium glutamicum* to Indole. *Microorganisms* 8, 1945. doi:10.3390/microorganisms8121945

Waskom, M., Gelbart, M., Botvinnik, O., Ostblom, J., Hobson, P., Lukauskas, S., et al. (2020). Seaborn: Statistical Data Visualization. *J. Open Source Softw.* 6 (60), 3021. doi:10.21105/joss.03021

Wehrs, M., Tanjore, D., Eng, T., Lievense, J., Pray, T. R., and Mukhopadhyay, A. (2019). Engineering Robust Production Microbes for Large-Scale Cultivation. *Trends Microbiol.* 27, 524–537. doi:10.1016/j.tim.2019.01.006

Wolf, S., Becker, J., Tsuge, Y., Kawaguchi, H., Kondo, A., Marienhagen, J., et al. (2021). Advances in Metabolic Engineering of *Corynebacterium glutamicum* to Produce High-Value Active Ingredients for Food, Feed, Human Health, and Well-Being. *Essays Biochem.* 65, 197–212. doi:10.1042/EBC20200134

Xiao, Z., Hou, X., Lyu, X., Xi, L., and Zhao, J.-y. (2014). Accelerated green Process of Tetramethylpyrazine Production from Glucose and Diammonium Phosphate. *Biotechnol. Biofuels* 7, 106. doi:10.1186/1754-6834-7-106

Yu, C., Simmons, B. A., Singer, S. W., Thelen, M. P., and VanderGheynst, J. S. (2016). Ionic Liquid-Tolerant Microorganisms and Microbial Communities for Lignocellulose Conversion to Bioproducts. *Appl. Microbiol. Biotechnol.* 100, 10237–10249. doi:10.1007/s00253-016-7955-0

Zhang, H., Li, Y., Wang, C., and Wang, X. (2018). Understanding the High L-valine Production in *Corynebacterium glutamicum* VWB-1 Using Transcriptomics and Proteomics. *Sci. Rep.* 8, 3632. doi:10.1038/s41598-018-21926-5

Zhou, Z., Wang, C., Xu, H., Chen, Z., and Cai, H. (2015). Increasing Succinic Acid Production Using the PTS-independent Glucose Transport System in a *Corynebacterium glutamicum* PTS-Defective Mutant. *J. Ind. Microbiol. Biotechnol.* 42, 1073–1082. doi:10.1007/s10295-015-1630-9